

# Influence of Zr Content in Ti-40Nb-xZr Alloys on the Microstructure, Elastic Modulus and Microhardness

Rafael Formenton Macedo dos Santos<sup>a\*</sup> , Carolina Neves Reis<sup>b</sup> , Conrado Ramos Moreira Afonso<sup>b</sup> 

<sup>a</sup>Universidade Federal de São Carlos (UFSCar), Programa de Pós-Graduação em Ciência e Engenharia de Materiais (PPG-CEM), 13.565-905, São Carlos, SP, Brasil.

<sup>b</sup>Universidade Federal de São Carlos (UFSCar), Departamento de Engenharia de Materiais (DEMa), 13.565-905, São Carlos, SP, Brasil.

Received: December 27, 2022; Revised: July 06, 2023; Accepted: July 17, 2023

In recent years, there has been a growing interest in the search for metallic alloys with favorable mechanical and chemical characteristics that elicit a positive biological response. Among these alloys,  $\beta$ -Ti alloys have attracted significant attention due to their low elastic modulus and excellent biocompatibility. The addition of Nb contributes to stabilizing the  $\beta$  phase at room temperatures, leading to the transformation of  $\beta$  into  $\beta + \alpha$  ( $\beta$ -isomorph). Additionally, despite Zr being commonly considered a neutral element, it can exhibit a  $\beta$ -stabilizing characteristic when combined with betagenic elements. Both Nb and Zr have been shown to effectively increase the lattice parameter of the  $\beta$  phase, which is advantageous for reducing the elastic modulus. The primary objective of this study was to characterize  $\beta$ -Ti alloys within the Ti-Nb-Zr system, specifically Ti-40Nb-20Zr, Ti-40Nb-30Zr, and Ti-40Nb-40Zr (wt.%) produced via arc furnace casting. The study aimed to investigate the influence of the proportion of  $\beta$ -stabilizing or betagenic elements on the microstructure and properties of the alloys, including Vickers microhardness and elastic modulus.

**Keywords:** Ternary  $\beta$ -Ti alloys, Elastic Modulus, Microstructure.

## 1. Introduction

The growth of the elderly population, the existence of degenerative bone diseases, and the occurrence of accidents represent a set of reasons to study metallic alloys that have mechanical and chemical characteristics favorable to the biological response<sup>1-3</sup>. In this context,  $\beta$ -Ti alloys are of interest due to their low elastic modulus and excellent biocompatibility<sup>1,2</sup>. Stress shielding is one of the mechanical problems associated with the difference in the values of the elastic modulus between the prosthesis material and the bone tissue<sup>4-7</sup>. In this case, this property value difference results in an uneven distribution of the mechanical stress, with most of the stress being directed toward the metal alloy. Thus, there is a reduction in the stimuli received by the tissue, causing interference in mechanotransduction, and resulting in problems such as atrophy and osteoporosis<sup>2,8,9</sup>.

Pure titanium shows a change in crystal structure from a temperature is known as  $\beta$ -transus (882°C)<sup>2,10</sup>. For lower temperatures, the material has a compact hexagonal structure (phase  $\alpha$ ); and for higher temperatures, a body-centered cubic structure ( $\beta$ -phase)<sup>1,2,10</sup>. The addition of alloying elements changes the  $\beta$ -transus temperature. So that the drop in the value of this transition temperature is equivalent to the enlargement of the beta phase field, thus elements with this character are called  $\beta$ -stabilizers<sup>1,2,10</sup>. Within this class of stabilizers, some elements decompose phase  $\beta$  into phase  $\beta +$  intermetallic ( $\beta$ -eutectoid) and those that transform the phase  $\beta$  into phase  $\beta +$  phase

$\alpha$  ( $\beta$ -isomorphs)<sup>1,2,10</sup>. Niobium is in the latter case<sup>1,2,11</sup>. On the other hand, zirconium is a neutral element, although it can express a  $\beta$ -phase stabilization behavior in the presence of  $\beta$ -stabilizers elements<sup>2,11,12</sup>. Both elements proved to be efficient in increasing the beta-phase lattice parameter, which is an indicative condition of reduced elastic modulus<sup>1,13,14</sup>.

Varying the amount of  $\beta$ -stabilizing elements added and changing the cooling rate result in different proportions of the phases obtained in the alloy<sup>2,10</sup>. Regarding beta Ti alloys, the amount of these elements added is significant, so that, regardless of the applied cooling rate, there is no alpha phase formation<sup>2</sup>. However, other phases are formed due to the non-occurrence of thermodynamic equilibrium. In this case, metastable phases known as  $\alpha'$ ,  $\alpha''$ ,  $\omega$ , and  $\beta'$  may be present<sup>1,2,10</sup>.

In a condition with a high concentration of alloying elements, small changes in the amount cause changes in the phases formed and, therefore, in their crystal structures. Comparatively, the formation of  $\alpha'$  (distorted HCP) and  $\alpha''$  (orthorhombic) is related to a lower content of added elements in contrast to the formation of a  $\omega$  and  $\beta'$ <sup>1,2,10</sup>. And, normally,  $\alpha'$  and  $\alpha''$  are phases that form without diffusion, that is, of the martensitic type<sup>1,10,14</sup>. Thus, there are two associated temperatures: the temperature at the beginning of the martensitic transformation ( $M_s$ ) and the temperature at the end of the martensitic transformation ( $M_f$ ), which can be changed with the addition of alloying elements and, therefore, are important for controlling the proportion of beta phase and martensitic phases formed<sup>1,2</sup>.

\*e-mail: [formentonrafael@gmail.com](mailto:formentonrafael@gmail.com)

When the alloying element concentration increases and the temperature at which the martensitic transformation starts is below room temperature, the beta phase can be fully retained<sup>1,2</sup>. However, normally, the formation of a metastable phase also occurs (phase  $\omega$  or phase  $\beta'$ ), which are regions of the material with a low concentration of alloying elements and with a high degree of distortion<sup>1,2,14,15</sup>. Furthermore, the formation of the omega phase can be associated with a non-diffusive process that occurs during a rapid cooling  $\omega_{\text{ath}}$  (athermal) or after a heat treatment through nucleation and growth  $\omega_{\text{iso}}$  (isothermal)<sup>1,2,10</sup>.

The formation of the athermal omega phase occurs from the collapse of some planes {222} of the beta phase in the  $\langle 111 \rangle$  directions, in order to form a single plane without the occurrence of diffusion and without changing the chemical composition of the original beta<sup>1,16</sup>. By increasing the concentration of Zr in alloys of the Ti-Nb-Zr system, a reduction in omega-phase precipitation was noted after rapid cooling. This fact is associated with the restriction imposed by this atom in the solution that makes it difficult to collapse the beta-phase planes, which are responsible for the phase transformation<sup>12,16,17</sup>. Therefore, the increase in Zr should reduce the value of the elastic modulus of the titanium alloy, as desired in the present work.

The microstructure will therefore be a consequence of the amount of alloying elements and the cooling conditions. Thus, the material's elastic modulus will be the contribution of the elastic modulus of each phase formed as a function of its volumetric fraction<sup>1,18</sup>. In this context, the search for reducing the value of this property can be estimated by models, which offer research perspectives to follow. Among them, there is the DV-X $\alpha$  method that has two analysis parameters:  $B_0$  and  $M_p$ , and based on a diagram of  $B_0$  (medium) x  $M_d$  (mean), it is possible to estimate the compositions of new research alloys that present the possibility of having a low elastic modulus<sup>1,2,19</sup>.

The parameters are averaged compositionally: parameter x atomic compositional fraction. For the case of the  $\beta$  phase, it was noted that the increase in  $B_0$  and the decrease in  $M_d$  are good indicators of stability, with  $B_0$  being the most appropriate parameter to analyze the reduction of the elastic modulus<sup>1,2,20</sup>. And when analyzing the influence of several elements, it was found that Nb and Zr are indicated as great elements for research. A better understanding of this method is beyond the scope of this study.

Finally, the main objective of the study is to characterize titanium beta alloys of the Ti-Nb-Zr system (Ti-40Nb-20Zr, Ti-40Nb-30Zr, Ti-40Nb-40Zr in wt.%) and investigate the influence of levels of  $\beta$ -stabilizing elements on the microstructure and properties, such as Vickers microhardness and elastic modulus, E (GPa), of alloys melted in an electric arc furnace. The alloys were named, respectively, as 20Zr, 30Zr, and 40Zr.

## 2. Methods

From high purity elements (>99.9%) and the master-alloy Ti-33Nb-33Zr (wt.%), acquired from ERCATA GmbH (Electron Beam Melting –EBM), the TNZ alloys system with different compositions of Ti, Nb, and Zr were obtained: Ti-40Nb-20Zr, Ti-40Nb-30Zr, Ti-40Nb-40Zr (wt.%), are presented in Table 1.

First, the arc furnace (Edmund Buhler model D-72411) was sanitized with ethyl alcohol to prevent contamination of the alloys with impurities. For sample preparation, a specific amount of Ti-33Nb-33Zr alloy was weighed and certain amounts of Ti, Nb, and Zr (Table 1) were thus added and placed in the furnace crucible. With the closing of the furnace, the purification of the atmosphere was started through a vacuum followed by an injection of argon, and this cycle was repeated three times. After the fourth injection, the alloys melting has begun. Finally, samples of approximately 20 g were obtained. The furnace was equipped with a water-cooled copper crucible. To ensure a homogeneous melt, the samples were turned inside the oven and melted 15 times.

Two cuts were made on each sample using diamond discs on the IsoMet 5000 precision cutter. The thinnest piece was used in the first part of the characterization (Olympus optical microscope (BX41M-LED model, with Infinity Capture acquisition and processing system) and the other piece was sent for XRD (Rigaku diffractometer, model Geigerflex ME210GF2, with sweep between the angles of 20 - 90° with a step of 2°/min). The cast (cut) samples were embedded in a cold-curing polymeric resin. Subsequently, they were sanded with 240, 360, 400, 600, 1200, and 1500 mesh sandpaper. And then, with the surface prepared for polishing, a polisher, and 0.3  $\mu\text{m}$  and 1  $\mu\text{m}$  alumina suspensions were used. Finally, the samples had their surfaces etched with a modified Kroll reagent (40% vol. HF + 40% vol. H<sub>2</sub>O + 20% vol. HNO<sub>3</sub>) for approximately 5 seconds.

Thus, it was possible to analyze them through the FEG microscope (Philips XL30) in SE and SEM-EDS modes, coupled to the Energy Dispersive Spectroscopy (EDS) system, with Oxford Link Tentafet X-ray detector for chemical composition semiquantitative determination. E (GPa) was determined by Sonelastic ATCP equipment following ASTM E1876:2001 and Vickers microhardness with a Shimadzu HMV-G20ST applying 0.5kgf for 15s following ASTM-E1019<sup>21,22</sup>.

The mathematical representation of the refraction phenomenon is given by Bragg's Law, where  $d_{\text{hkl}}$ : interplanar distance, n: reflection order,  $\theta$ : diffraction angle; and  $\lambda$ : wavelength. For each crystal system there is an expression for  $d_{\text{hkl}}$  to the lattice parameters and to the Miller indices (hkl)<sup>23</sup>.

**Table 1.** Mass amount of Ti-33Nb-33Zr alloy and high purity element (Ti, Nb, and Zr) used to obtain each of the 20Zr, 30Zr and 40Zr alloys (wt.%).

Alloys/ Elements	Ti-33Nb-33Zr (g)	Ti (g)	Nb (g)	Zr (g)
20Zr	12	4	4	0
30Zr	18	0	2	0
40Zr	12	0	4	4

(I) Bragg's law:  $n\lambda = 2d_{hkl} \cdot \sin(\theta)$

(II) Interplanar distance to cubic system:  $d_{hkl} = \frac{a}{\sqrt{h^2 + k^2 + l^2}}$

### 3. Results

The results of the tests and analysis described in the previous section will be presented below, and then a discussion will be presented regarding the present results.

#### 3.1. Microstructure characterization

##### 3.1.1. X-ray Diffraction (XRD)

Figure 1 show the X-ray patterns of the four alloys studied, indicating only the presence of  $\beta$ -Ti phase (bcc) for 20Zr, 30Zr, and 40Zr. The XRD technique has a detection limitation, that is, for sufficiently low volumetric fractions (below 5% in volume) and precipitate sizes, no peaks are displayed in the diffractogram even if the phase is present. In this way, the conclusion of phases formed through XRD analysis is insufficient for the identification of  $\omega$ -phase since this phase is usually in very small volume and in nanometric scale for 20Zr, 30Zr, 40Zr alloys, as showed in the literature<sup>24-27</sup>. In this case, from the analysis of the results of measurements of hardness and elastic modulus, it will be possible to indicate the presence of such phase, since both properties mentioned are influenced by the occurrence of  $\omega$ -phase, increasing them.

It can be seen from the diffraction pattern that the increase in the zirconium content shifts all peaks to values smaller than  $2\theta$ , indicating an increase in the lattice parameter, and this is reported in the literature<sup>13,28</sup>. As widely observed in the literature, (110) peak was identified in this work, the main peak for the beta phase, with greater intensity. In addition to these, (200), (211), and (220) peaks were also identified, and these planes are characteristic of the  $\beta$ -Ti (bcc) phase.

Based on the literature, the lattice parameter of the  $\beta$  phase, at 900°C, for pure Ti is  $a = 3.332 \text{ \AA}$ <sup>29</sup>. In addition, from the X-ray pattern and Bragg's law and the interplanar distance equation, it was possible to obtain the values of the  $\beta$ -phase lattice parameter for each alloy ( $a_{20Zr} = 3.3479$ ;  $a_{30Zr} = 3.3672$ ;  $a_{40Zr} = 3.3938 \text{ \AA}$ ) confirming that there was an increase of lattice parameter of the  $\beta$  phase with increasing Zr addition. Thus, as previously mentioned, it was noticed that all alloys presented higher lattice parameter values when compared to the pure Ti parameter. This result was already expected since the presence of Zr was shown by the literature as being efficient in increasing the lattice parameter<sup>1,2,10,13</sup>. Thus, being an indication of the reduction in the value of the elastic modulus.

##### 3.1.2. Optical (OM) and scanning electron microscopy (SEM).

The chemical composition of the alloys was analyzed through semi-quantitative EDS analysis. Bearing in mind that SEM-EDS is a semi-quantitative technique, and therefore a small variation is expected, the results obtained show that the alloys then have the designed chemical composition. Table 2 shows the chemical composition of each alloying element considering atomic percentage (at.%) and weight (wt.%).

Figure 2 shows a sequence of optical micrographs (left) and SEM micrographs (right). As in the XRD, in the optical microscope, there is a limitation regarding identifying phases with nanometric sizes since the device's resolution is approximately 400 nm. Therefore, for alloys 20Zr, 30Zr, and 40Zr, even if the phase is present, it will not be possible to observe it. It can be noted in all alloys the typical dendritic microstructure of solidification.

During solidification, even at higher rates of cooling, the outermost solidified layer follows the nominal equilibrium composition. Therefore, there are compositional fluctuations between the liquid phase and the solid phase formed as the temperature is lowered<sup>30</sup>. Moreover, when the content of  $\beta$ -stabilizing elements is high, there is a tendency for microsegregation to occur during solidification, which can lead to an ill-defined  $\beta$ -Transus<sup>31</sup>. In this way, the composition of the dendrites varies slightly from that of the matrix, even though both have a body-centered cubic structure, as pointed out by the XRD (for alloys 20Zr, 30Zr, and 40Zr). This justifies the contrast obtained in the OM images since each region presents different corrosion resistances, which generate different visual aspects after metallographic preparation.

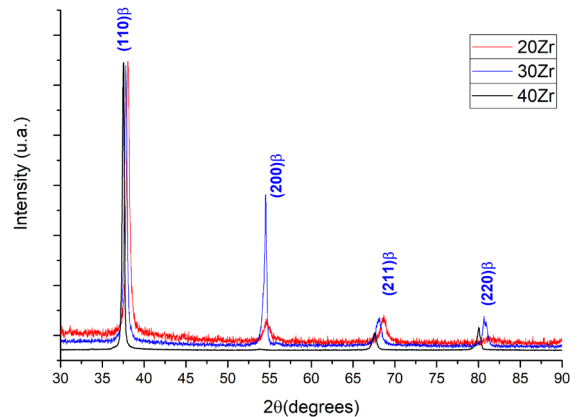


**Figure 1.** X-ray diffraction patterns for the Ti-40Nb-20Zr, Ti-40Nb-30Zr, and Ti-40Nb-40Zr in the "as-cast" condition.

**Table 2.** Semi-quantitative chemical composition obtained by SEM-EDS (weight %) for 20Zr, 30Zr, and 40Zr, considering weight percentage (wt.%) and atomic (at.%).

Alloys/ Elements	Zr wt. % - (at. %)	Nb wt. % - (at. %)	Ti wt. % - (at. %)
20Zr	23 - (17)	37 - (26.8)	40 (56.2)
30Zr	30 - (23.4)	38 - (29.1)	32 (47.5)
40Zr	38 - (33.8)	41 - (34)	21 (32.2)

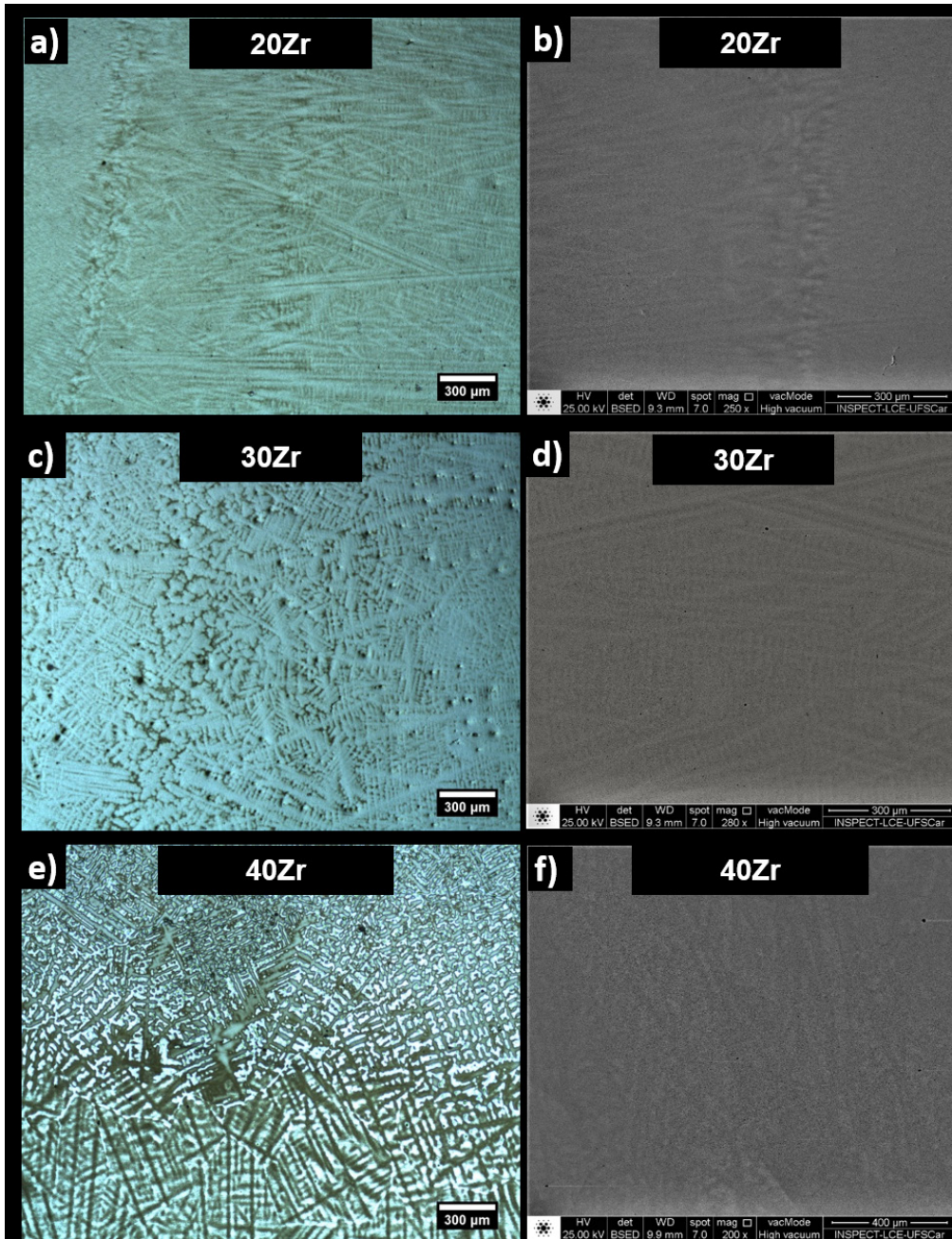


**Figure 2.** Micrographs obtained by OM (left) and SEM (right) a),b) 20Zr, c),d) 30Zr and e),f) 40Zr in as-cast condition.

### 3.2. ThermoCalc, elastic modulus and vickers microhardness

The ThermoCalc software provided pseudo-binary diagrams for each of the alloys indicating the volumetric variation of the phases as a function of temperature under equilibrium conditions. Thus, there is no indication of metastable phases formation such as  $\omega$ , and  $\beta'$ . Therefore, ThermoCalc was used to follow the microstructural evolution during solidification, and to estimate the  $\beta$ -transus temperature. Thus, it could be noticed that in all cases there was a decrease in the  $\beta$ -transus

of the 20Zr, 30Zr, and 40Zr alloys related to the transition temperature for pure Ti (882°C), showing an expansion of the  $\beta$ -phase field, as a result of the presence of the  $\beta$ -stabilizing elements, Table 3.

Table 3 shows the values of lattice parameter of  $\beta$  phase (Å), elastic modulus, E (GPa),  $\beta$ -Transus (°C) and Vickers microhardness obtained for each of the studied alloys, with the remarkable influence of Zr addition. The addition of this  $\beta$ -stabilizing element reduces the elastic modulus value and increases the vickers microhardness value simultaneously. These data are graphically represented in Figure 3.

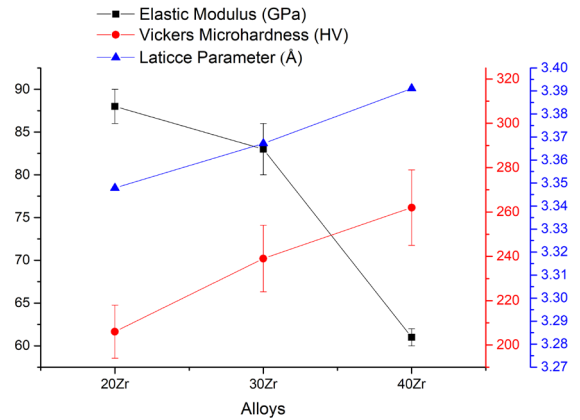
**Table 3.** Experimental results for Ti-40Nb-20Zr, Ti-40Nb-30Zr, and Ti-40Nb-40Zr.

Parameters/Results	20 Zr	30 Zr	40 Zr
Crystal lattice parameter ( $\beta$ phase) ( $\text{\AA}$ )	3.3479	3.3672	3.3938
$\beta$ -Transus ( $^{\circ}\text{C}$ )	510	490	480
Elastic Modulus	$88 \pm 2$	$83 \pm 3$	$61 \pm 1$
Vickers Microhardness	$206 \pm 12$	$239 \pm 15$	$262 \pm 17$

When the 20Zr ( $\text{Ti}_{56.3}\text{Nb}_{29.0}\text{Zr}_{14.7}$ ) 30Zr ( $\text{Ti}_{45.2}\text{Nb}_{31.1}\text{Zr}_{23.7}$ ) e 40Zr ( $\text{Ti}_{32.5}\text{Nb}_{33.5}\text{Zr}_{34.0}$ ) alloys are compared (in at.%), at first it is possible to have an impression that Zr itself showed an  $\beta$ -stabilizer effect, since it is observed, that with the Zr addition, there is a decrease in the  $\beta$ -transus temperature. However, differently to what is observed, although there is maintenance of Nb content (wt.%), the Zr content varies in atomic percentage (Zr at.%). As Nb and Zr form substitutional solid solution with Ti in  $\beta$ -Ti alloys, from the point of view of the atomic percentage (at.%), an increase in the Nb atomic fraction is observed when we add Zr. This effect is observed, since Zr, due to its higher atomic number ( $Z = 40$ ) than the Ti ( $Z = 22$ ), when Zr is added to the alloy it increases, relatively, the Nb at.%, consequently stabilizing  $\beta$ -Ti phase (bcc) phase at lower temperatures. Therefore, the decrease in  $\beta$ -transus is associated with an increase in the number of Nb atoms as a consequence of the Zr addition, but it can be said that Zr shows a  $\beta$ -stabilizing effect just when combined with a typical  $\beta$ -stabilizing element, such as Nb. This is true because only binary Ti-Zr alloys would never form  $\beta$ -Ti phase (bcc), regardless of Zr fraction added to Ti, resulting only in equilibrium  $\alpha$ -Ti phase (hcp)<sup>32</sup>.

The increasing addition of  $\beta$ -stabilizing elements, Zr, proved to be efficient in increasing the lattice parameter, which was already expected based on the literature<sup>1-3,10</sup>. Thus, with the distancing of the atoms present in the body-centered cubic structure (beta phase), the interatomic force was reduced and, consequently, there was a drop in the values of the elastic modulus with the increase of this element in the solid solution. Comparing the alloys with the presence of Zr, increasing the concentration of this element proved to be efficient in reducing the elastic modulus.

In contrast, there was an increase in Vickers microhardness as the Zr content increased, probably due to the solid solution hardening mechanism<sup>33,34</sup>. That is, the progressive addition of Zr contributed to the expansion of bcc crystal structure (increasing lattice parameter) becoming increasingly distorted by the difference in atomic ratio and, in this way, generating more internal strain in the crystalline structure in atomic scale. As a macroscopic response, the material indicated an increase in microhardness. As previously commented, Zr hinders the omega phase precipitation increasing stabilization of  $\beta$ -Ti phase (bcc). Therefore, it is to be expected that the main reason for the increase in hardness in the 20Zr, 30Zr, and 40Zr alloys are due to solid solution hardening. Finally, further analysis is needed using high-energy monochromatic synchrotron XRD and transmission electron microscopy (TEM) in high-resolution mode (HRTEM) and using selected area electron diffraction (SAD)<sup>35</sup>.

**Figure 3.** Variation of elastic modulus, Vickers microhardness and  $\beta$ -phase lattice parameter for the 20Zr, 30Zr, and 40Zr alloys.

#### 4. Conclusion

For Ti-40Nb-40Zr alloy, with the highest Zr content lead to greater value of  $\beta$  lattice parameter for  $\beta$ -Ti phase (bcc) in solid solution with Ti resulting in the lowest elastic modulus  $E = 61$  GPa and the highest value of Vickers microhardness of 262 HV, due to solid solution hardening.

The combined  $\beta$ -stabilizer effect of Zr together with Nb lead to increased atomic fraction of Nb (decreasing Ti content), decreasing  $\beta$ -transus temperature, increasing lattice parameter of  $\beta$ -Ti phase (bcc) and suppressing metastable  $\omega$  precipitation.

Combined effects of increasing lattice parameter and electronic parameters ( $B_o \times M_d$ ) confirms that increasing Zr addition to in  $\beta$ -Ti Ti-40Nb-xZr ( $x = 20, 30$  and 40wt.%) alloys increased Vickers microhardness of 262 HV, indicating increased mechanical strength and leading to the lowest elastic modulus  $E = 61$  GPa for as-cast biomedical metallic alloys applications.

#### 5. Acknowledgements

This study was financed in part by the Coordenação de Aperfeiçoamento de Pessoal de Nível Superior - Brasil (CAPES) - Finance Code 001. The authors would like to thank Brazilian agencies CNPq Universal Project #422015/2018-0 (C.R.M.A.). To CAPES - Coordenação de Aperfeiçoamento de Pessoal de Nível Superior for the financial support to carry out this work with a grant process n° 88887.371759/2019-00 (R.F.M.S.). To FAPESP – “The State of São Paulo Research Foundation” for the financial support to carry out this work with “Projeto Temático” n° 2018/18293-8, and Scientific Initiation (IC) FAPESP Grant n° 2020/12431-0 (C.N.R.)

## 6. References

- Gonzalez ED, Afonso CRM, Nascente PAP. Influence of Nb content on the structure, morphology, nanostructure, and properties of Titanium-Niobium magnetron sputter deposited coatings for biomedical applications. *Surf Coat Technol.* 2017;326(Part B):424-8. <https://doi.org/10.1016/j.surfcoat.2017.03.015>.
- Santos RFM, Ricci VP, Afonso CRM. Continuous cooling transformation (CCT) diagrams of  $\beta$  Ti-40Nb and TMZF alloys and influence of cooling rate on microstructure and elastic modulus. *Thermochim Acta.* 2022;717:179341. <http://dx.doi.org/10.1016/j.tca.2022.179341>.
- Niinomi M. Recent research and development in titanium alloys for biomedical applications and healthcare goods. *Sci Technol Adv Mater.* 2003;4(5):445-54. <http://dx.doi.org/10.1016/j.stam.2003.09.002>.
- Afonso CRM, Aleixo GT, Ramirez AJ, Caram R. Influence of cooling rate on microstructure of Ti-Nb alloy for orthopedic implants. *Mater Sci Eng C.* 2007;27(4):908-13. <http://dx.doi.org/10.1016/j.msec.2006.11.001>.
- Ricci VP, Santos RFM, Asato GH, Roche V, Jorge AM Jr, Afonso CRM. Assessment of anodization conditions and annealing temperature on the microstructure, elastic modulus, and wettability of  $\beta$ -Ti40Nb alloy. *Thin Solid Films.* 2021;737:138949. <http://dx.doi.org/10.1016/j.tsf.2021.138949>.
- Geetha M, Singh AK, Asokamani R, Gogia AK. Ti based biomaterials, the ultimate choice for orthopedic implants – a review. *Prog Mater Sci.* 2009;54(3):397-425. <http://dx.doi.org/10.1016/j.pmatsci.2008.06.004>.
- Bobyn JD, Mortimer ES, Glassman AH, Engh CA, Miller JE, Brooks CE. Producing and avoiding stress shielding: laboratory and clinical observations of noncemented total hip arthroplasty. *Clin Orthop Relat Res.* 1992;(274):79-96.
- Gusmão CVB, Belangero WD. Como a célula óssea reconhece o estímulo mecânico? *Rev Bras Ortho.* 2009;44(4):299-305. <http://dx.doi.org/10.1590/S0102-36162009000400003>.
- Nagels J, Stokdijk M, Rozing PM. Stress shielding and bone resorption in shoulder arthroplasty. *J Shoulder Elbow Surg.* 2003;12(1):35-9. <http://dx.doi.org/10.1067/mse.2003.22>.
- Aleixo GT, Afonso CRM, Coelho AA, Caram R. Effects of omega phase on elastic modulus of Ti-Nb alloys as a function of composition and cooling rate. *Diffus Defect Data Solid State Data Pt B Solid State Phenom.* 2008;138:393-8. <http://dx.doi.org/10.4028/www.scientific.net/SSP.138.393>.
- Lütjering G, Williams JC. *Titanium.* Berlin: Springer; 2003.
- Abdel-Hady M, Fuwa H, Hinoshita K, Kimura H, Shinzato Y, Morinaga M. Phase stability change with Zr content in  $\beta$ -type Ti-Nb alloys. *Scr Mater.* 2007;57(11):1000-3. <http://dx.doi.org/10.1016/j.scriptamat.2007.08.003>.
- Yu Z, Yuxuan L, Xianjin Y, Zhenduo C, Shengli Z. Influence of Zr content on phase transformation, microstructure and mechanical properties of  $Ti_{75-x}Nb_{22}Zr_x$  ( $x=0-6$ ) alloys. *J Alloys Compd.* 2009;486(1-2):628-32. <http://dx.doi.org/10.1016/j.jallcom.2009.07.006>.
- Dobromyslov AV, Elkin VA. Martensitic transformation and metastable  $\beta$ -phase in binary titanium alloys with d-metals of 4-6 periods. *Scr Mater.* 2001;44(6):905-10. [http://dx.doi.org/10.1016/S1359-6462\(00\)00694-1](http://dx.doi.org/10.1016/S1359-6462(00)00694-1).
- Froes FH, Yolton CF, Capenos JM, Wells MGH, Williams JC. The relationship between microstructure and age hardening response in the metastable beta titanium alloy Ti-11.5 Mo-6 Zr-4.5 Sn (beta III). *Metall Trans A, Phys Metall Mater Sci.* 1980;11:21-31. <http://dx.doi.org/10.1007/BF02700435>.
- Pang EL, Pickering EJ, Baik SI, Seidman DN, Jones NG. The effect of zirconium on the omega phase in Ti-24Nb-[0-8] Zr (at.%) alloys. *Acta Mater.* 2018;153:62-70. <http://dx.doi.org/10.1016/j.actamat.2018.04.016>.
- Zheng Y, Williams REA, Nag S, Banerjee R, Fraser HL, Banerjee D. The effect of alloy composition on instabilities in the beta phase of titanium alloys. *Scr Mater.* 2016;116:49-52. <http://dx.doi.org/10.1016/j.scriptamat.2016.01.024>.
- Santos RFM, Rossi MC, Vidilli AL, Borrás VA, Afonso CRM. Assessment of  $\beta$  stabilizers additions on microstructure and properties of as-cast  $\beta$  Ti-Nb based alloys. *J Mater Res Technol.* 2022;22:3511-24. <http://dx.doi.org/10.1016/j.jmrt.2022.12.144>.
- Morinaga M, Kato M, Kamimura T, Fukumoto M, Harada I, Kubo K. Theoretical design of  $\beta$ -type titanium alloys. *JOM.* 1993;1-2:217-24.
- Abdel-Hady M, Hinoshita K, Morinaga M. General approach to phase stability and elastic properties of  $\beta$ -type Ti-alloys using electronic parameters. *Scr Mater.* 2006;55(5):477-80. <http://dx.doi.org/10.1016/j.scriptamat.2006.04.022>.
- ASTM: American Society for Testing and Materials. ASTM E1876-15: standard test method for dynamic Young's modulus, shear modulus, and Poisson's ratio by impulse excitation of vibration. West Conshohocken: ASTM International; 2015.
- ASTM: American Society for Testing and Materials. ASTM E384-17: standard method for microindentation hardness of materials. West Conshohocken: ASTM International; 2017.
- Callister WD, Rethwisch DG. *Materials science and engineering: an introduction.* 9th ed. Hoboken: Wiley; 2014. Chapter 3, The structure of crystalline solids; p. 51-104.
- Santos RFM, Ricci VP, Afonso CRM. Influence of swaging on microstructure, elastic modulus and Vickers microhardness of beta Ti-40Nb alloy for implants. *J Mater Eng Perform.* 2021;30(5):3363-9. <http://dx.doi.org/10.1007/s11665-021-05706-3>.
- Nunes ARV, Gabriel SB, Nunes CA, Araújo LS, Baldan R, Mei P et al. Microstructure and mechanical properties of Ti-12Mo-8Nb alloy hot swaged and treated for orthopedic applications. *Mater Res.* 2017;20(2):526-31. <http://dx.doi.org/10.1590/1980-5373-MR-2017-0637>.
- Dey GK, Tewari R, Banerjee S, Jyoti G, Gupta SC, Joshi KD et al. Formation of a shock deformation induced  $\omega$  phase in Zr 20 Nb alloy. *Acta Mater.* 2004;53(18):5243-54. <http://dx.doi.org/10.1016/j.actamat.2004.07.008>.
- Banerjee S, Tewari R, Dey GK. Omega phase transformation – morphologies and mechanisms. *Int J Mater Res.* 2006;97(7):963-77. <http://dx.doi.org/10.1515/ijmr-2006-0154>.
- Gonzalez ED, Fukumasu NK, Afonso CRM, Nascente PAP. Impact of Zr content on the nanostructure, mechanical, and tribological behaviors of  $\beta$ -Ti-Nb-Zr ternary alloy coatings. *Thin Solid Films.* 2021;721:138565. <http://dx.doi.org/10.1016/j.tsf.2021.138565>.
- Leyens C, Peters M. *Titanium and titanium alloys: fundamentals and applications.* Weinheim: Wiley-VCH; 2005. 532 p.
- Porter DA, Easterling KE, Sherif MY. *Phase transformations in metals and alloys.* 3rd ed. Boca Raton: CRC Press; 2009. Chapter 4, Solidification: alloy solidifications; p. 209-29.
- Banerjee D, Pilchak AL, Williams JC. Processing, structure, texture and microtexture in titanium alloys. *Mater Sci Forum.* 2012;710:66-84. <http://dx.doi.org/10.4028/www.scientific.net/MSF.710.66>.
- Takahashi M, Kikuchi M, Okumo O. Grindability of dental cast Ti-Zr alloys. *Mater Trans.* 2009;50(4):859-63. <http://dx.doi.org/10.2320/matertrans.MRA2008403>.
- Baloyi R. Investigation into the effect of solid solution chemistry on lattice parameters and microstructural properties of  $\beta$ -Ti alloys [dissertation]. Johannesburg: University of the Witwatersrand; 2010. 94 p.
- Zhang F, Weidmann A, Nebe BJ, Burkel E. Preparation of TiMn alloy by mechanical alloying and spark plasma sintering for biomedical applications. *J Phys Conf Ser.* 2009;144:012007. <http://dx.doi.org/10.1088/1742-6596/144/1/012007>.
- Afonso CRM, Ferrandini PL, Ramirez AJ, Caram R. High resolution transmission electron microscopy study of the hardening mechanism through phase separation in a  $\beta$ -Ti-35Nb-7Zr-5Ta alloy for implant applications. *Acta Biomater.* 2010;6:1625-9. <http://dx.doi.org/10.1016/j.actbio.2009.11.010>.